Magnetic and electrical properties of $GdNi_{1-x}Cu_x$ compounds

1992 J. Phys.: Condens. Matter 4 8233

(http://iopscience.iop.org/0953-8984/4/42/012)

J. Phys.: Condens. Matter 4 (1992) 8233–8244. Printed in the UK

Magnetic and electrical properties of $GdNi_{1-x}Cu_x$ compounds

J A Blanco†‡, J C Gómez Sal†, J Rodríguez Fernandez†, D Gignoux‡, D Schmitt‡ and J Rodríguez-Carvajal§

† DCITTYM, Facultad de Ciencias, Universidad de Cantabria, 39005 Santander, Spain
‡ Laboratoire Louis Néel, CNRS, 166X, 38042 Grenoble, France
§ Institut Laue–Langevin, 156X, 38042 Grenoble, France

Received 22 April 1992

Abstract. The magnetic properties of the orthorhombic compounds $GdNi_{1-x}Cu_x$ have been studied by means of magnetization, resistivity and neutron diffraction measurements. GdNi and $GdNi_{0.7}Cu_{0.3}$ show ferromagnetic structures while for $GdNi_{0.4}Cu_{0.6}$ we propose a helimagnetic structure. The link between the macroscopic magnetic properties in the ordered phase and the magnetic structures is also stressed. Comparison with other $RNi_{1-x}Cu_x$ compounds with strong magnetocrystalline anisotropy allows one to clarify the role of the magnetic interactions as well as the importance of the magnetocrystalline anisotropy in all these pseudo-binary compounds.

1. Introduction

The equiatomic RNi (R ≡ rare-earth) compounds have crystallographic structures built up from trigonal prisms with the rare earth being in the corner and the nickel at the centre. The different arrangements of these prisms lead to several crystallographic structures. The orthorhombic CrB-type structure (space group, $Cmcm$) exists for compounds with light rare earths (La, Ce, Pr, Nd and Gd) while the orthorhombic FeB-type structure (space group, $Pnma$) appears for the heavy-rare-earth compounds (Dy to Tm). TbNi is an intermediate monoclinic phase. In all these structures, the rare-earth atoms lie in very-low-symmetry sites. The stability of this sequence of structures was qualitatively explained by steric considerations [1] depending on the ratio of the volume of the transition-metal atoms to the volume of the rare-earth atoms ($r = V_M/V_R$). For the smallest values of r, the CrB-type structure is stable but, when nickel atoms are replaced by larger copper atoms, r increases and the FeB-type structure will be established. For instance this occurs for 10% Cu in TbNi while 20% Cu is needed in the GdNi case.

From the magnetic point of view, the substitution of Ni by Cu modifies the RKKY interactions and a change from ferromagnetic to antiferromagnetic behaviour has been observed with increasing amount of Cu [2]. Only the rare-earth ions are magnetic in these systems. The crystalline-electric-field (CEF) effects have been investigated in compounds with $L \neq 0$ [2]. In the antiferromagnetic compounds, sine-wave-modulated structures were found just below T_N. They were interpreted as due to the existence of competing RKKY interactions in the presence of strong magnetocrystalline anisotropy which imposes a well defined crystallographic direction for the magnetic moments. These modulated structures could remain stable down to very

0953-8984/92/428233+12$04.50

low temperatures for the non-Kramers ions ($HoNi_{0.5}Cu_{0.5}$ [2] and $TbNi_{0.6}Cu_{0.4}$ [3]) because the low-symmetry CEF leads to a non-magnetic singlet or must transform into equal-moment structures at low temperatures for Kramers ions such as Er^{3+} ($ErNi_{0.6}Cu_{0.4}$) [4] owing to the existence of a magnetic doublet ground state.

In the above-mentioned work [2] an initial study of the magnetic properties of the $GdNi_{1-x}Cu_x$ compounds gave $x = 0.35$ as the crossover point for the ferromagnetic–antiferromagnetic behaviour and recently the magnetic structures of some of these compounds have been presented [5]. The aim of the present paper is to discuss the magnetic properties of $GdNi_{1-x}Cu_x$ compounds from the magnetization, resistivity and neutron diffraction results, bearing in mind previous results on other $RNi_{1-x}Cu_x$. In the gadolinium case with $L = 0$, the CEF effects are very small and it will be possible to stress the role of the magnetic interactions and then, by comparison with the $L \neq 0$ rare-earth compounds, discuss the importance of the magnetocrystalline anisotropy on the $RNi_{1-x}Cu_x$ systems.

2. Experimental details

Polycrystalline samples of $GdNi_{1-x}Cu_x$ for $x = 0$, 0.3 and 0.6 were prepared by direct fusion of the stoichiometric amounts of constituents in a cold-crucible induction furnace. The crystalline structures were checked by x-ray analysis, being CrB type for GdNi and FeB type for $GdNi_{0.7}Cu_{0.3}$ and $GdNi_{0.4}Cu_{0.6}$.

The bulk magnetic measurements were performed using the extraction method under magnetic fields of up to 80 kOe in the temperature range 1.5–300 K at the Laboratoire Louis Néel, Grenoble. The resistivity was measured by the AC four-probe method between 1.8 and 300 K at the Laboratorio de Física de la Materia Condensada, Universidad de Cantabria, Santander. Neutron diffraction experiments were performed on the D4B diffractometer at the Institute Laue–Langevin, Grenoble. The neutron wavelength was $\lambda = 0.5$ Å in order to reduce the absorption cross section of Gd at higher wavelengths. A typical counting time was 8 h per diffractogram. The diffraction patterns were collected at 4.2 and 90 K. The analysis of the data was done using the programs existing in the STRAP package [6, 7]. The refinements of the crystallographic and magnetic structures were carried out using the Rietveld method.

3. Magnetic measurements

Figures 1, 2 and 3 show the magnetization curves at different temperatures for GdNi, $GdNi_{0.7}Cu_{0.3}$ and $GdNi_{0.4}Cu_{0.6}$, respectively. The first two have clear ferromagnetic behaviour. At 1.5 K, for fields higher than 15 kOe, the magnetization saturation is almost reached, being 7.1 μ_B per Gd atom at 80 kOe for both GdNi and $GdNi_{0.7}Cu_{0.3}$. On the contrary, $GdNi_{0.4}Cu_{0.6}$ shows an antiferromagnetic behaviour. The magnetization curves (figure 3) show a critical field which is around 20 kOe at 1.5 K, decreasing when the temperature increases and disappearing above $T_N = 63$ K. The saturation value cannot be reached even for fields higher than 80 kOe. The spontaneous magnetization of the ferromagnetic compounds was deduced from Arrott plots. Its thermal variation is compared in figure 4 with the theoretical variation obtained from the Brillouin law $B_{7/2}(x)$. We have also obtained the Curie temperatures which are 69 K

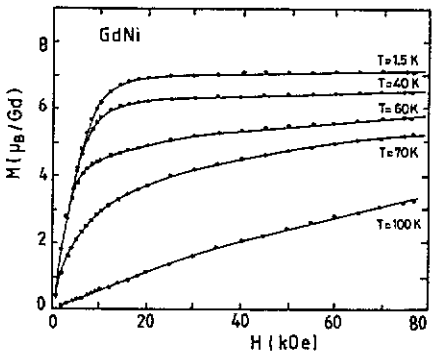

Figure 1. Magnetization curves of GdNi.

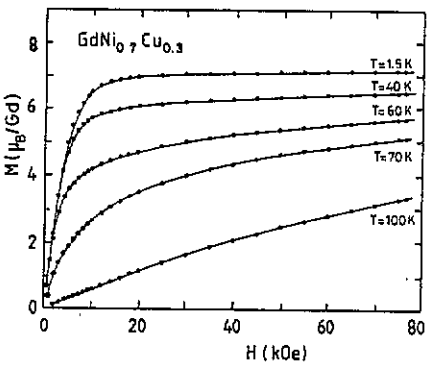

Figure 2. Magnetization curves of $GdNi_{0.7}Cu_{0.3}$.

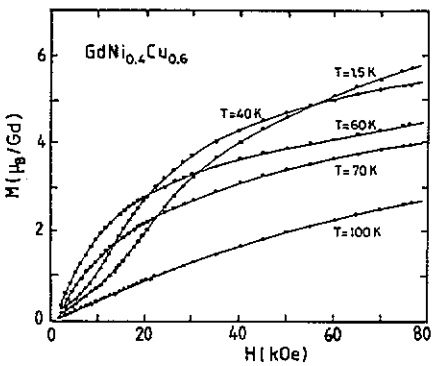

Figure 3. Magnetization curves of $GdNi_{0.4}Cu_{0.6}$.

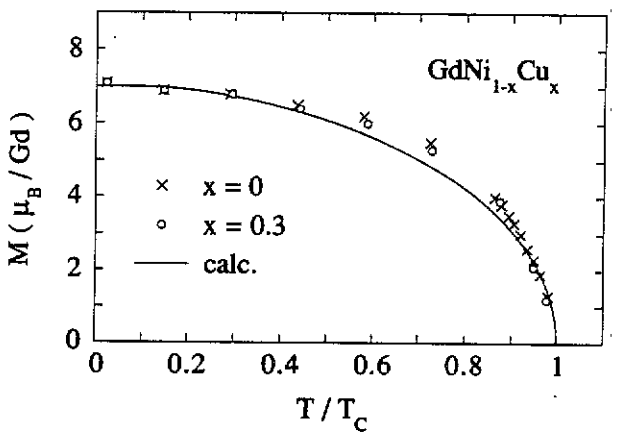

Figure 4. Extrapolated saturation magnetization versus temperature for GdNi and $GdNi_{0.7}Cu_{0.3}$ compared with the theoretical $B_{7/2}$ Brillouin function.

and 68 K for GdNi and $GdNi_{0.7}Cu_{0.3}$, respectively. In these two compounds the modifications of the RKKY interactions when Ni is substituted by Cy should compensate for the crystalline structure change, leading to very similar T_c values.

The thermal variation in the reciprocal susceptibility is presented in figure 5. For $GdNi_{0.4}Cu_{0.6}$, $1/\chi$ has a minimum at the Néel temperature (63 K). At higher temperatures the three compounds follow the Curie–Weiss law. The effective moment

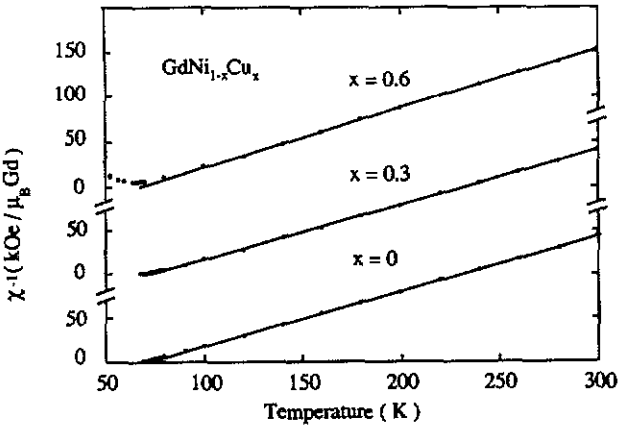

Figure 5. Reciprocal susceptibility versus temperature for $GdNi_{1-x}Cu_x$, $x = 0, 0.3$ and 0.6: ——, Curie–Weiss law, taking into account the corrections explained in the text.

deduced from the Curie constant are 8.41 μ_B per Gd atom, 8.48 μ_B per Gd atom and 8.24 μ_B per Gd atom for $x = 0, 0.3$ and 0.6, respectively; these values are noticeably larger than the value of 7.94 μ_B per Gd atom expected for the free ion value. These large values have also been found for other Gd-based compounds [8, 9] and could be related to conduction band effects which become apparent in two different ways: one is the presence of a constant term χ_0 from the Pauli paramagnetism, and the other is an enhancement of the Gd magnetic moment associated with conduction electron polarization close to the magnetic ion. These effects lead to a modified Curie–Weiss law $\chi = \chi_0 + C(1+\alpha)^2/(T - \Theta_p)$, where C is the free-ion Curie constant and α is a phenomenological parameter describing the polarization effect. With these corrections we obtain negligible values of χ_0 and $\alpha = 6.7 \times 10^{-2}$, 5.8×10^{-2} and 0.4×10^{-2} for $x = 0, 0.3$ and 0.6, respectively, which have the same order of magnitude as those found in other rare-earth–nickel compounds [10].

The paramagnetic Curie temperatures Θ_p are positive and very close to each other, even for the $GdNi_{0.4}Cu_{0.6}$ antiferromagnetic compound ($\Theta_p \simeq 69$ K). This high positive value for Θ_p indicates that the exchange interactions have strong positive components although the long-range magnetic order is antiferromagnetic ($T_N = 63$ K). In the absence of CEF effects, the deviations from the Curie–Weiss law at temperatures just above T_c or T_N are due to short-range spin correlations. The main characteristics of the magnetic properties of these compounds are shown in table 1.

Table 1. Magnetic properties of the $GdNi_{1-x}Cu_x$ compounds investigated.

x	T_c (K)	T_N (K)	Θ_p (K)	α ($\times 10^{-2}$)	μ_{eff} (μ_B)	Magnetization (μ_B) at 1.5 K and 80 kOe
0	69		74	6.7	8.41	7.1
0.3	68		75	5.8	8.48	7.1
0.6		63	69	3.9	8.24	5.7

4. Electrical resistivity measurements

As was noted previously for GdNi [11, 12], the $GdNi_{1-x}Cu_x$ samples are very brittle. This produces two effects on the resistivity measurements: the first is the presence

of cracks, leading to high values of the resistivity; the second is the possible cracks propagation phenomenon, especially in the high-temperature range, leading to a non-negligible dispersion of the ρ(300 K) values before and after successive thermal cycles (300 K–4.2 K–300 K). For each composition the electrical resistivity has been measured on at least two different pieces from different batches, in order to select the curve showing the higher value of the resistivity ratio RR=ρ(300 K)/ρ(4.2 K) and less crack propagation. In figure 6 we report the experimental resistivity curves for the different $GdNi_{1-x}Cu_x$ as well as for LaNi and YNi. The general behaviour is characteristic of metallic magnetic compounds; the changes in the slope correspond to the ordering temperatures (71 K, 70 K and 64 K) which are very close to those determined from magnetic measurements. The values obtained for the residual resistivities are 0.9 $\mu\Omega$ cm, 145.9 $\mu\Omega$ cm and 165.6 $\mu\Omega$ cm for $x = 0$, 0.3 and 0.6, respectively. It is worth mentioning that the high values of residual resistivity ρ_{res} for the diluted compounds could be mainly influenced by the disorder in the transition-metal site substitution, as has been observed for other pseudo-binary compounds [13].

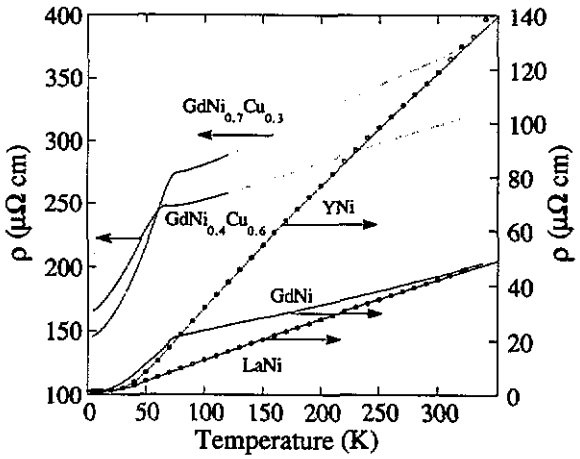

Figure 6. Thermal variation in the electrical resistivities of $GdNi_{1-x}Cu_x$, $x = 0, 0.3$ and 0.6, and LaNi and YNi. Note the two scales used.

The estimation of the magnetic contribution to the total resistivity is a complicated task in samples with cracks propagation. Our criteria were as follows:

(i) The experimental resistivities of the LaNi (space group, $Cmcm$) and YNi (space group, $Pnma$) non-magnetic isomorphous compounds have been fitted to the Grüneisen–Bloch law (full curves in figure 6), leading to Debye temperatures Θ_D of 180 K and 230 K, respectively. Considering the mass difference correction [14] we obtain $\Theta_D = 170$ K for GdNi and $\Theta_D = 190$ K for $GdNi_{0.7}Cu_{0.3}$ and $GdNi_{0.4}Cu_{0.6}$, respectively; these values are close to $\Theta_D = 182$ K proposed for the RNi [15] compounds.

(ii) Because of the cracks the experimental curves were multiplied by a constant K in order to obtain the paramagnetic slopes β found in a similar isomorphous series RPt [16], being $\beta = 0.073$ $\mu\Omega$ cm K^{-1} for CrB-type and 0.125 $\mu\Omega$ cm K^{-1} for FeB-type compounds.

(iii) With the Θ_D and β-values we have estimated the Grüneisen–Bloch law corresponding to the phonon contribution ρ_{phon} for each compound. The magnetic resistivity is obtained from $\rho_{mag} = (\rho - \rho_{res})K - \rho_{phon}$. This procedure is especially

appropriate for Gd compounds which have quite small CEF effects. In figure 7 we show the magnetic resistivities compared with those of the GdPt (FeB-type) compound without cracks.

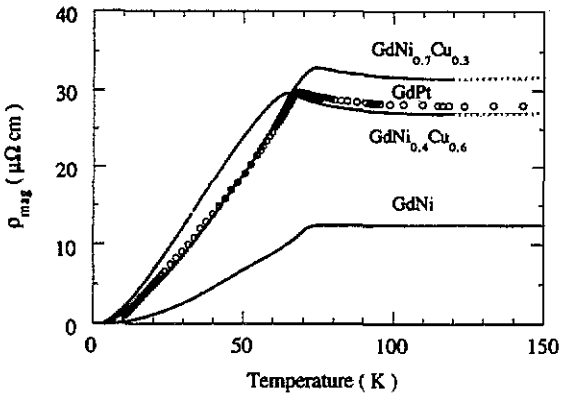

Figure 7. Thermal variation in the magnetic contribution to the resistivity of $GdNi_{1-x}Cu_x$, $x = 0, 0.3$ and 0.6, and GdPt.

The ρ_{mag} (T) curves show a decrease at temperatures just higher than the critical temperature T_c before reaching the ρ_{mo} saturation value, giving rise to a peak at around T_c. This behaviour reveals the existence of short-range-order magnetic correlations [17] between Gd ions.

Our final comment is about the $\rho_{mag}(T)$ variation below T_c. In figure 8 is presented $\rho_{mag}(T)/\rho_{mag}(T_c)$ versus T/T_c. For GdNi, $GdNi_{0.7}Cu_{0.3}$ and GdPt the shapes of the curves are almost the same. On the contrary, $GdNi_{0.4}Cu_{0.6}$ presents quite a different behaviour, showing a curvature change at about $T/T_c = 0.5$.

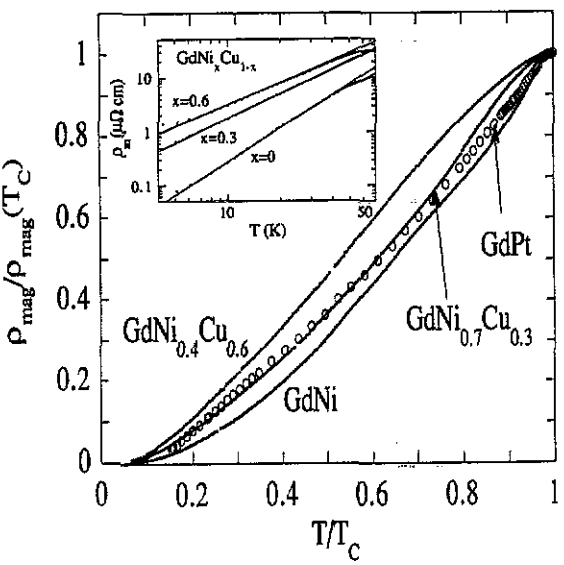

Figure 8. Reduced magnetic resistivity $\rho_{mag}/\rho_{mag}(T_c)$ versus T/T_c for $GdNi_{1-x}Cu_x$, $x = 0, 0.3$ and 0.6, and GdPt (T_c is the critical temperature). The inset shows a log–log plot of the low-temperature $\rho_m \sim T^n$ behaviour: ——, fits with $n = \frac{4}{3}, \frac{3}{2}$ and 2, for $x = 0.6, 0.3$ and 0, respectively.

The inset of figure 8 shows the best low-temperature fittings of ρ_{mag} to T^n laws, in a log–log plot. The exponents obtained are 2, $\frac{3}{2}$ and $\frac{4}{3}$ for $x = 0$, 0.3 and 0.6, respec-

tively. The $n = 2$ exponent appears from the spin waves in ferromagnetic systems [18] and was also found for GdNi by other workers [11–13]. The $n = \frac{3}{2}$ value observed for $GdNi_{0.7}Cu_{0.3}$ was also found for GdPt [16] and in dilute $Gd_xLa_{1-x}Ni$ compounds for $0.4 \leqslant x \leqslant 0.7$ [13]. The unexpected $n = \frac{4}{3}$ exponent found for the antiferromagnetic $GdNi_{0.4}Cu_{0.6}$, which has not been obtained for intermetallic compounds as far as we know, reflects the more complex magnetic structure of this compound.

5. Magnetic structures

The magnetic structures of GdNi, $GdNi_{0.7}Cu_{0.3}$ and $GdNi_{0.4}Cu_{0.6}$ have been determined by means of neutron diffraction measurements [5]. The patterns obtained at 90 K for GdNi and $GdNi_{0.7}Cu_{0.3}$ are characteristic of the CrB-type (space group, $Cmcm$) and FeB-type (space group, $Pnma$) crystallographic structures, respectively. In both compounds, at 4.2 K (figure 9) no new peaks appear but only a supplementary contribution to some of the nuclear peaks is observed. The features observed in the $y_{obs} - y_{calc}$ difference pattern are due to some degree of preferred orientation caused by the relatively coarse grains. The best Rietveld refinement for the magnetic intensities corresponds to a Fy (+,+,+,+) mode in the two cases, leading to collinear ferromagnetic structures with the magnetic moments lying in the b direction (figure 10). As can be seen from this figure the b directions in the two structures are not equivalent, even though they are derived from one another. The results of the refinements are summarized in table 2.

Table 2. Characteristics of the magnetic structures of $GdNi_{1-x}Cu_x$ compounds.

	GdNi	$GdNi_{0.7}Cu_{0.3}$	$GdNi_{0.4}Cu_{0.6}$
Crystallographic structure type	CrB	FeB	FeB
Cell parameters at 4.2 K			
a (Å)	3.778	7.116	7.177
b (Å)	10.365	4.312	4.931
c (Å)	4.221	5.486	5.490
Atomic positions	y(Gd), 0.140 y(Ni), 0.428	x(Gd), 0.181 z(Gd), 0.133 x(Ni, Cu), 0.037 z(Ni, Cu), 0.627	x(Gd), 0.183 z(Gd), 0.133 x(Ni, Cu), 0.035 z(Ni, Cu), 0.628
R Bragg factor (%)	7.2	4.9	5.1
Magnetic structure	Ferromagnetic	Ferromagnetic	Helimagnetic
Propagation vector q	(0,0,0)	(0,0,0)	(0,0,0.25)
Moment direction	[010]	[010]	⊥[001]
Magnetic moment value $M_0(\mu_B)$	7.3 ± 0.1	7.1 ± 0.1	7.0 ± 0.1
R_{mag} (%)	7.8	7.6	6.1

The patterns obtained at 90 and 4.2 K for $GdNi_{0.4}Cu_{0.6}$ are displayed in figure 11. The 90 K patterns again correspond to the FeB (space group, $Pnma$) structure, but at 4.2 K new peaks appear which are well indexed with a propagation vector $q = (0, 0, \frac{1}{4})$, confirming the antiferromagnetic character of this compound. The magnetic intensities have been calculated for two kinds of magnetic moment arrangement.

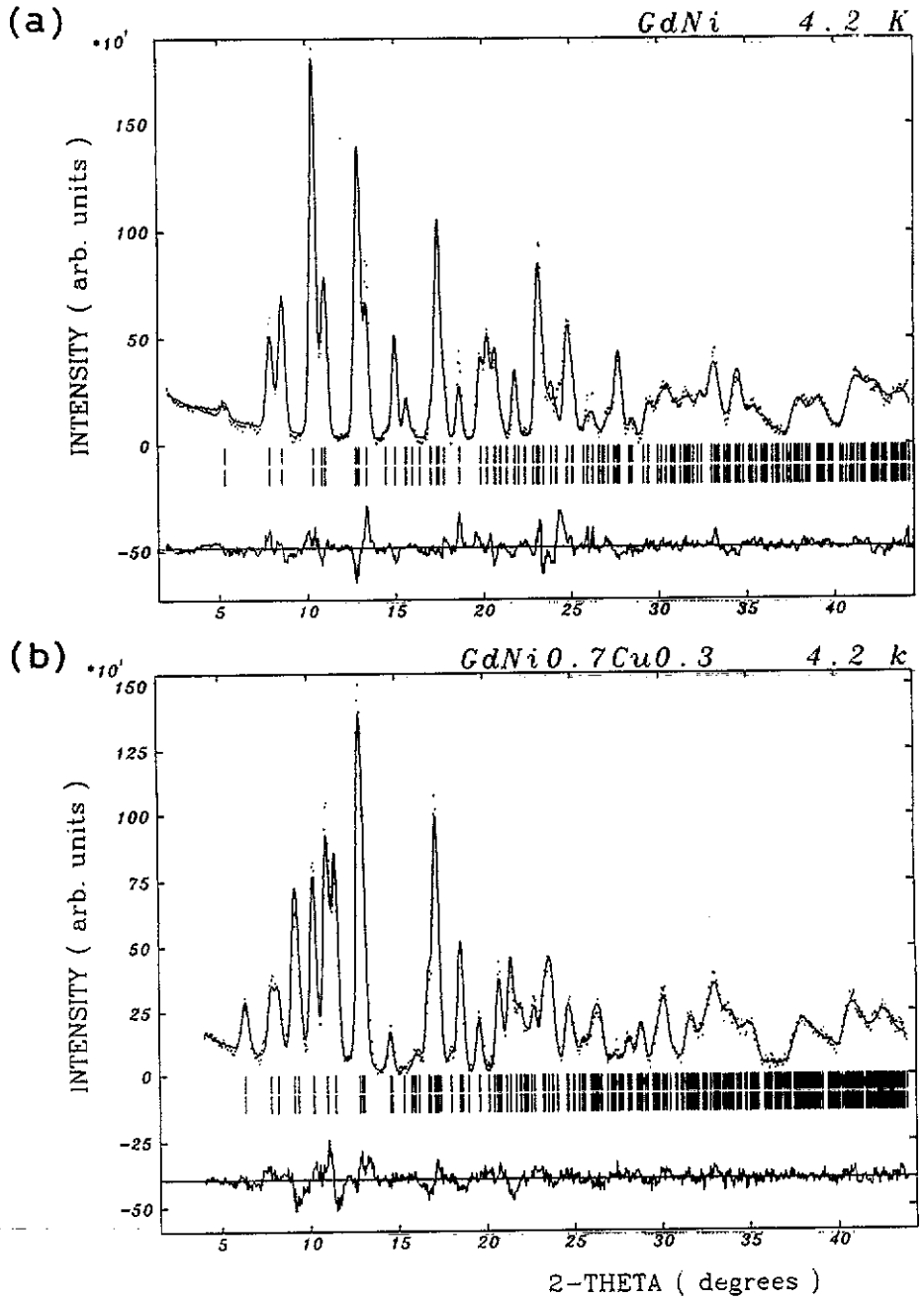

Figure 9. Neutron diffraction patterns of GdNi and $GdNi_{0.7}Cu_{0.3}$ at 4.2 K: ——, Rietveld refinements; the upper vertical marks are the nuclear peaks, and the lower vertical marks are the magnetic peaks.

(i) The first set of calculations was made considering a helimagnetic configuration, and the best Rietveld refinement is obtained for the moments lying in the (a, b) plane.

(ii) Another refinement was carried out for sinusoidally modulated structures. In

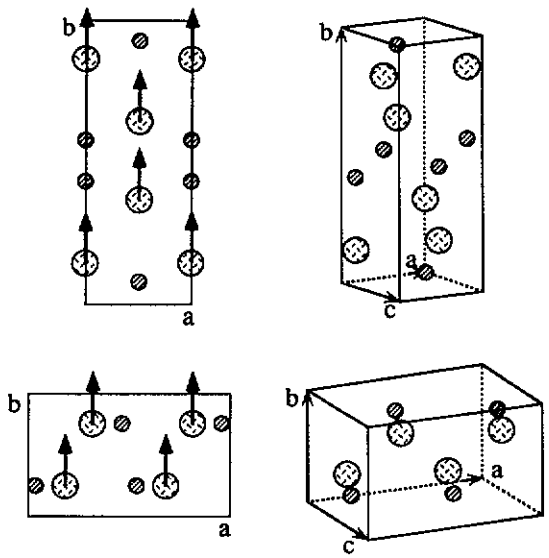

Figure 10. Magnetic structures of GdNi (CrB type) and $GdNi_{0.7}Cu_{0.3}$ (FeB type). The structures are projected on the corresponding (a, b) plane.

this case, the moments were found to lie in a particular direction of the (a, b) plane.

However, at 4.2 K an equal-moment structure should have been established owing to the Kramers character of the Gd^{3+} ion. Therefore, the modulated structure must evolve to an antiphase structure at low temperatures, giving rise to $\pm 3q$ and $\pm 5q$ harmonics. In particular, a $(0,0,0)^{\pm 3q}$ peak is expected to appear at $2\theta = 3.9°$. The absence of such satellites in the 4.2 K pattern makes the helimagnetic solution more likely. This magnetic structure is shown in figure 12. The best agreement between the observed and calculated intensities R_{mag} (6%) is obtained for moments $M_j = 7\{\cos[2\pi(\boldsymbol{q}\cdot\boldsymbol{r}_j)\hat{\boldsymbol{x}}] + \sin[2\pi(\boldsymbol{q}\cdot\boldsymbol{r}_j)]\ \hat{\boldsymbol{y}}\}$ (in Bohr magnetons), where the $\hat{x}$ and $\hat{y}$ directions are the unitary vectors along a and b, and r_j is the atomic position. From one crystalline cell to the next along the c direction the moments are rotated 90° in the (a, b) plane. The 360° rotation is achieved with four crystalline cells which form the new magnetic lattice. In table 2 are presented the results fo the Rietveld refinements for this compound.

6. Discussion

As occurs in the other RNi_xCu_{1-x} systems the substitution of Ni by Cu in GdNi modifies the conduction electron concentration and gives rise to an increase in the negative interactions, leading to a change from a ferromagnetic behaviour to an antiferromagnetic behaviour. This change appears at about $x = 0.35$.

For the $L \neq 0$ rare-earth-based ferromagnetic compounds it has been shown that the strong CEF effects force the magnetic moments to be in the (a, c) plane, in both the CrB-type [19, 20] and the FeB-type [21] structures. However, for GdNi and $GdNi_{0.7}Cu_{0.3}$ the magnetic moments lie in the b direction. A second-order CEF could be responsible [22] for this easy-magnetization direction, although anisotropic exchange interactions must not be disregarded.

For the antiferromagnetic compounds, the Fourier transform of the exchange interactions $J(q)$ has a maximum value for q different from zero and thus incommen-

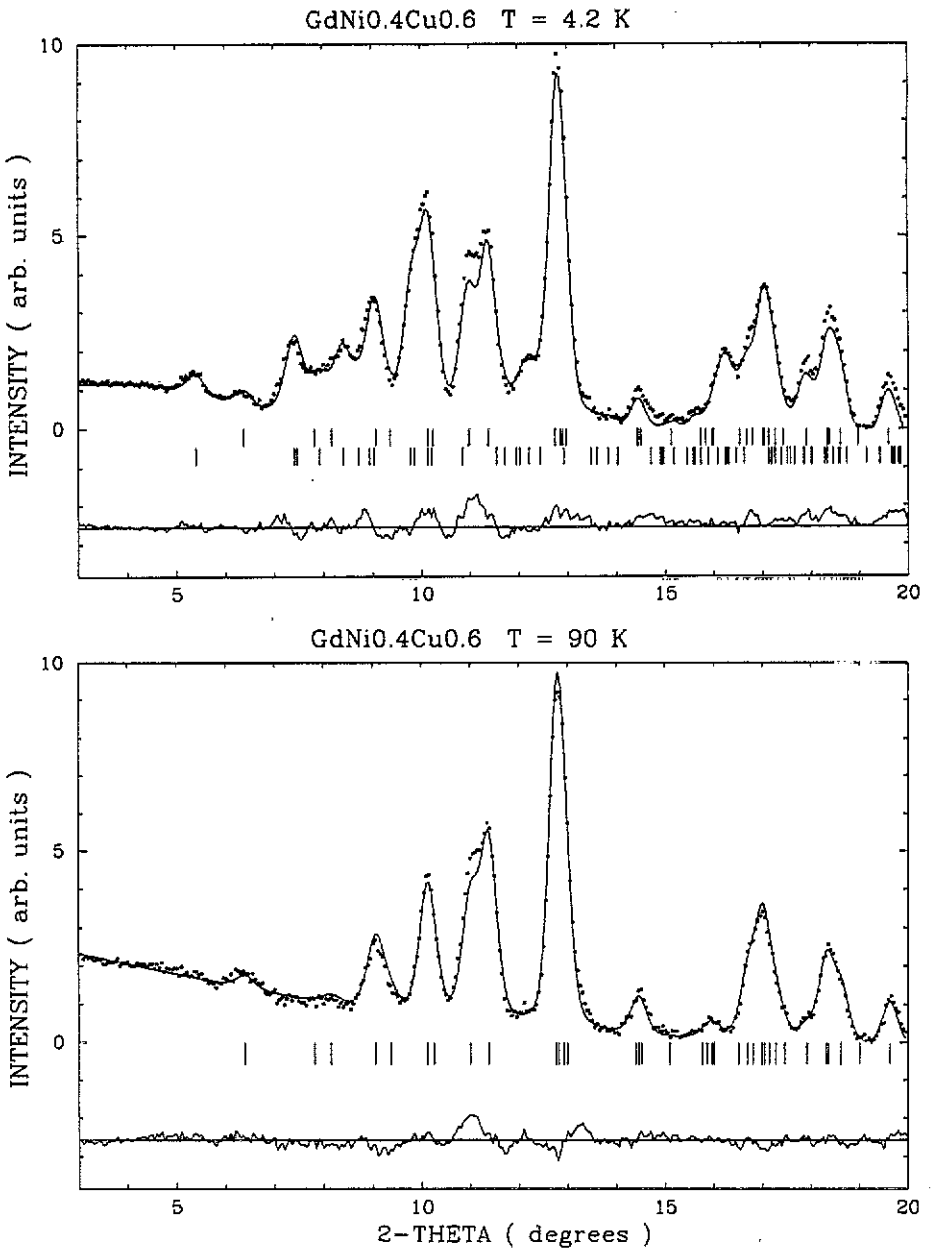

Figure 11. Neutron diffraction patterns for $GdNi_{0.4}Cu_{0.6}$ at 90 and 4.2 K.

surate magnetic structures can be stabilized. In fact, two types of propagation vector q have been experimentally found: one is about $q = (0, 0.14, 0)$ for $TbNi_{0.6}Cu_{0.4}$ and $ErNi_{0.6}Cu_{0.4}$ and the second is close to $q = (0, 0, 0.25)$ for $HoNi_{0.5}Cu_{0.5}$ and $GdNi_{0.4}Cu_{0.6}$. This change in the q-value and direction could be understood at least qualitatively as due to the modification of $J(q)$, when the Cu content increases. It is worth noticing that $q = (0, 0, 0.25)$ appears for higher Cu concentrations. The confirmation of such a hypothesis will need a complete study of the magnetic structures

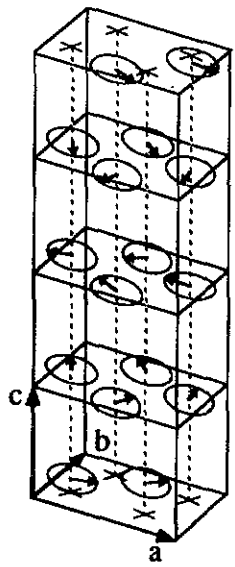

Figure 12. The helimagnetic structure of $GdNi_{0.4}Cu_{0.6}$.

for a wider range of concentrations x.

For the $L \neq 0$ compounds the strong magnetocrystalline anisotropy imposes the magnetic moment direction and the antiferromagnetic structures are sine wave modulated (non-Kramers ions) or antiphase at low temperatures (Kramers ions). On the contrary, in gadolinium-based compounds an equal-moment helimagnetic structure seems to be more likely, the moments lying in the (a, b) plane perpendicular to the propagation vector as in a simple helimagnetic structure.

The $GdNi_{1-x}Cu_x$ system is an appropriate example for stressing the link between the macroscopic magnetic properties in the ordered phase and the magnetic structures especially for $GdNi_{0.4}Cu_{0.6}$.

In GdNi, the magnetization (figure 4), the susceptibility (figure 5) and the magnetic resistivity ($\rho_{mag} \sim T^2$) exhibit the expected behaviour corresponding to the simple collinear ferromagnetic structure. $GdNi_{0.7}Cu_{0.3}$ shows the same magnetic behaviour, but the magnetic resistivity follows a $T^{3/2}$ law. This fact, together with the anomalous resistivity peak at around T_c (figure 7) which is greater than for GdNi, suggests that for $x = 0.3$ the magnetic fluctuations play an important role, even at temperatures much lower than T_c

As is well known for antiferromagnetic compounds, the macroscopic polycrystalline measurements can only give us some indication about what kinds of complex magnetic structure appear; in particular in Gd-based compounds it is rather difficult to distinguish between helical and modulated arrangements. The magnetization processes are quite similar for both structures and they are characterized by soft transitions with the magnetic field and saturation fields H_c, often with high values. This is the case for $GdNi_{0.4}Cu_{0.6}$ ($H_s \simeq 120$ kOe), $GdCu_6$ ($H_s = 240$ kOe) [23] and $GdGa_2$ ($H_s = 220$ kOe) [24], among other compounds. These high H_c values show the difficulty in destroying the magnetic structure because of the importance of the exchange interactions.

As can be seen in figure 8 the shape of the $\rho_{mag}/\rho_{mag}(T_c)$ versus T/T_c curve for $GdNi_{0.4}Cu_{0.6}$ is quite different from that for the ferromagnetic compounds, showing

a faster variation at low temperatures. This is related to a more complex magnetic structure associated with a larger entropy, as has been commented on in previous studies [25, 26]. The influence of magnetic fluctuations seems to be enhanced, as could be deduced from the highest peak at around T_N and the lowest coefficient of the $\rho_{mag} \sim T^n$ law.

The specific heat measurement now in progress will provide us with a new test for the existence of the helimagnetic structure or the antiphase structure. Indeed, recent calculations of the magnetic specific heat for Gd-based compounds [27], using the mean-field approximation, should allow us to distinguish between equal-moment or amplitude-modulated structures close to the ordering temperatures.

Acknowledgments

We gratefully acknowledge J M Barandiarán for the facilities for preparing the samples at the Laboratorio of the Universidad del País Vasco. This work is supported by the Comisión Interministerial de Ciencia y Tecnología (grant MAT-90, 0877-C02-01).

References

[1] Klepp K and Parthe E 1982 *J. Less-Common Met.* **85** 181
[2] Gignoux D and Gómez Sal J C 1976 *J. Magn. Magn. Mater.* **1** 203
[3] Gignoux D, Lemaire R and Paccard D 1972 *Phys. Lett.* **41A** 187
[4] Gignoux D and Gómez Sal J C 1974 *Phys. Lett.* **50A** 63
[5] Blanco J A, Gignoux D, Gómez Sal J C, Rodríguez-Carvajal J, Rodríguez Fernández J and Schmitt D 1992 *Physica* B **181** 100
[6] Rodríguez-Carvajal J, Mand A and Pannetier J 1987 *Institut Laue–Langevin Internal Report* 87 RO 14T
[7] Rodríguez-Carvajal J 1991 *FULL PROF, Satellite Meet. 15th Cong. of the International Union of Crystallography (Toulouse, 1991)* p 127
[8] Barandiarán J M, Gignoux D, Rodríguez Fernández J and Schmitt D 1989 *Physica* B **154** 293
[9] Hiebl K and Rogl P 1985 *J. Magn. Magn. Mater.* **50** 39
[10] Barthem V M T S, Gignoux D, Nait-Saada A, Schmitt D and Creuzet G 1988 *Phys. Rev.* B **37** 1733
[11] Mori K and Sato K 1980 *J. Phys. Soc. Japan* **49** 246
[12] Zimm C B, Steward W F, Barclay J A, Campenni C K, Overton W, Olsen C, Harding D, Chesebrough R and Johanson W 1988 *Adv. Cryogenic Eng.* **33** 791
[13] Gratz E, Hilscher G, Sassik H and Sechovsky V 1986 *J. Magn. Magn. Mater.* **54–7** 459
[14] Meaden G T 1965 *Electrical Resistance of Metals* (New York: Plenum)
[15] Mori K and Sato K 1982 *Proc. 3rd Int. Conf. on Ferrites (Kyoto, 1980)* (Dordrecht: Reidel)
[16] Gómez Sal J C, Rodríguez Fernández J, López Sánchez R J and Gignoux D 1986 *Solid State Commun.* **59** 117
[17] de Gennes P. G. and Friedel J. 1958 *J. Phys. Chem. Solids* **4** 71
[18] Manari I 1956 *Prog. Theor. Phys.* **16** 58
[19] Lemaire R and Paccard D 1970 *Les Elements de Terres Rares* vol II (Paris: CNRS) p 231
[20] Castets A, Gignoux D, Gómez Sal J C and Roudaut E 1982 *Solid State Commun.* **44** 1329
[21] Gignoux D 1974 *J. Physique* **35** 455
[22] Sato K, Koyachi K and Mori K 1981 *J. Appl. Phys.* **52** 2084
[23] Takayanaga S, Onuko Y, Ina K, Komatsubara T, Wada W, Watanabe T, Sakakibara T and Goto T 1989 *J. Phys. Soc. Japan* **58** 1031
[24] Gignoux D and Schmitt D 1991 *J. Magn. Magn. Mater.* **100** 99
[25] Barandiarán J M, Gignoux D, Schmitt D, Gómez Sal J C and Rodríguez Fernández J 1987 *J. Magn. Magn. Mater.* **69** 61
[26] Blanco J A, Gignoux D, Gómez Sal J C, Rodríguez Fernández J and Schmitt D 1992 *J. Magn. Magn. Mater.* **104–7** 1285
[27] Blanco J A, Gignoux D Schmitt D 1991 *Phys. Rev.* B **43** 13145